Induction of Columnar Discotic Behavior in Verdazyl Radicals with Alkylsulfanyl Substituents

Aleksandra Jankowiak [a] , Damian Pociecha [b] , Hirosato Monobe [c] ,
Jacek Szczytko [d] , Żaneta Dębska [e] , Jarosław Romański [e] & Piotr
Kaszyński [a] [e]

[a] Department of Chemistry , Vanderbilt University , Nashville , TN ,
37235 , USA

[b] Department of Chemistry , University of Warsaw , 02-089 Warsaw ,
Poland

[c] Faculty of Physics , University of Warsaw , Hoża 69, 00-681
Warsaw , Poland

[d] National Institute of Advanced Industrial Science and Technology,
AIST Kansai Centre , Ikeda , Osaka 563-8577 , Japan

[e] Faculty of Chemistry , University of Łódź , Tamka 12, 91403 , Łódź
, Poland
Accepted author version posted online: 25 Oct 2012.Published
online: 29 May 2013.

PLEASE SCROLL DOWN FOR ARTICLE

instructions, formulae, and drug doses should be independently verified with primary sources. The publisher shall not be liable for any loss, actions, claims, proceedings, demand, or costs or damages whatsoever or howsoever caused arising directly or indirectly in connection with or arising out of the use of this material.

Taylor & Francis
Taylor & Francis Group

INDUCTION OF COLUMNAR DISCOTIC BEHAVIOR IN VERDAZYL RADICALS WITH ALKYLSULFANYL SUBSTITUENTS

Aleksandra Jankowiak,[1] Damian Pociecha,[2] Hirosato Monobe,[3] Jacek Szczytko,[4] Żaneta Dębska,[5] Jarosław Romański,[5] and Piotr Kaszyński[1,5]

[1]*Department of Chemistry, Vanderbilt University, Nashville, TN 37235, USA*
[2]*Department of Chemistry, University of Warsaw, 02-089 Warsaw, Poland*
[3]*Faculty of Physics, University of Warsaw, Hoża 69, 00-681 Warsaw, Poland*
[4]*National Institute of Advanced Industrial Science and Technology, AIST Kansai Centre, Ikeda, Osaka 563-8577, Japan*
[5]*Faculty of Chemistry, University of Łódź, Tamka 12, 91403 Łódź, Poland*

GRAPHICAL ABSTRACT
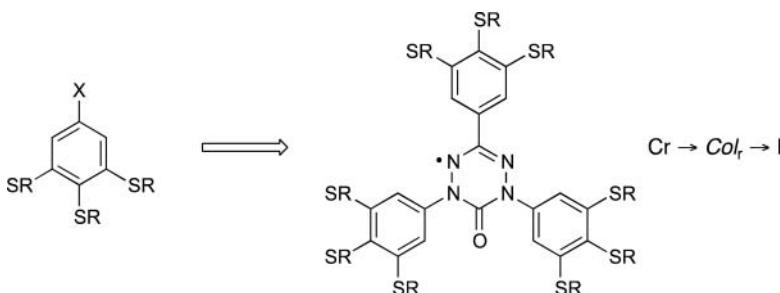
Abstract *Substitution of the 1,3,5-triphenyl-6-oxoverdazyl radical with n-alkylsulfanyl groups lead to derivatives **1[n]**, which exhibit a columnar rectangular phase (Col$_r$) below 60 °C. Compounds **1[n]** have a broad absorption band in the visible region with maxima at 540 and 610 nm and redox potentials $E^{0/+1}_{1/2} = +0.99$ V and $E^{0/-1}_{1/2} = -0.45$ V vs. SCE. Time-of-flight (TOF) investigation of **1[8]** revealed hole mobility of $\mu_h = 1.52 \times 10^{-3}$ cm^2 V^{-1} s^{-1} in the columnar phase with an activation energy $E_a = 0.06 \pm 0.01$ eV. Magnetization studies of **1[8]** demonstrated nearly ideal paramagnetic behavior in both solid and fluid phases above 200 K and weak antiferromagnetic interactions at low temperatures. Verdazyl derivatives **1[n]** were prepared in a sequence of reactions starting from 1-bromo-3,4,5-trifluorobenzene by alkylsulfanylation, followed by hydrazinylation, and finally 6-oxoverdazyl ring assembly using the Milcent method.*

Address correspondence to Dr Piotr Kaszynski, Department of Chemistry, Vanderbilt University, Nashville, TN 37235, USA. E-mail: piotr.kaszynski@vanderbilt.edu

INTRODUCTION

One-dimensional charge transport along the self-assembled columns in discotic liquid crystals is a desirable property for applications in molecular electronics[1] and light harvesting devices.[2,3] Therefore, a number of aromatic and heteroaromatic discotic mesogens have been investigated for their photophysical properties.[4] More facile generation of an electron-hole pair is expected in neutral π-radicals than in closed-shell aromatics due to their relatively high-lying SOMO and low I_p.[5] Recently, first examples of liquid crystalline π delocalized stable radicals, derived from the triphenylmethyl, were reported.[6] This discovery provided new impetus for the development of other materials of this type, in which magnetic properties can be coupled with anisotropic charge transport, dielectric switching, chirality, and photo-alignment.

Verdazyls,[7] including 6-oxoverdazyls, are among several π-delocalized stable radicals. They exhibit broad absorption bands in the visible part of the spectrum and an electrochemical window of about 1.5 V.[8] Some verdazyl derivatives have been investigated as components of paramagnetic semiconductors,[9] and in photo-excited molecular systems[10] intended for photo-magnetic devices.[11] With this in mind have prepared a series of discotic derivatives of 6-oxoverdazyl **1[n]** (Chart 1) and investigated their liquid crystalline, electrochemical, magnetic, and photovoltaic properties.[12]
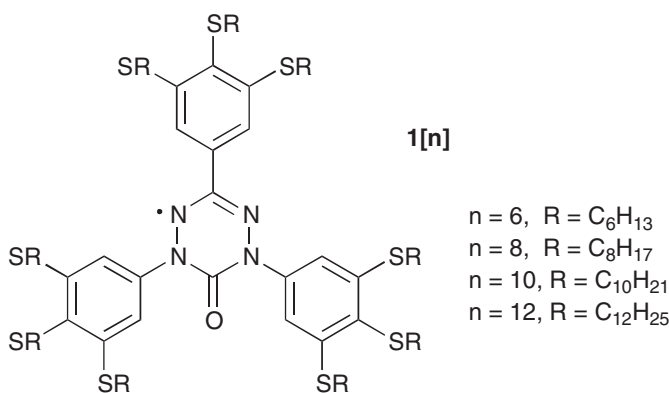

$$n = 6, \ R = C_6H_{13}$$
$$n = 8, \ R = C_8H_{17}$$
$$n = 10, \ R = C_{10}H_{21}$$
$$n = 12, \ R = C_{12}H_{25}$$

Chart 1

RESULTS AND DISCUSSION

Synthesis. Radicals **1[n]** were obtained from hydrazines **2[n]**[13] and benzaldehydes **3[n]**[14] according to the Milcent method[15] (Scheme 1). Thus, crude hydrazines were converted to hydrazones **4[n]**, which were reacted with triphosgene to give carbonyl chlorides **5[n]**. After isolation and purification, the chlorides were reacted with hydrazine **2[n]** in benzene. The resulting tetrazanes **6[n]** were partially purified and oxidized with $K_3Fe(CN)_6$ under PTC conditions or with PbO_2 to give radicals **1[n]** in 10–20% overall yield.[12]
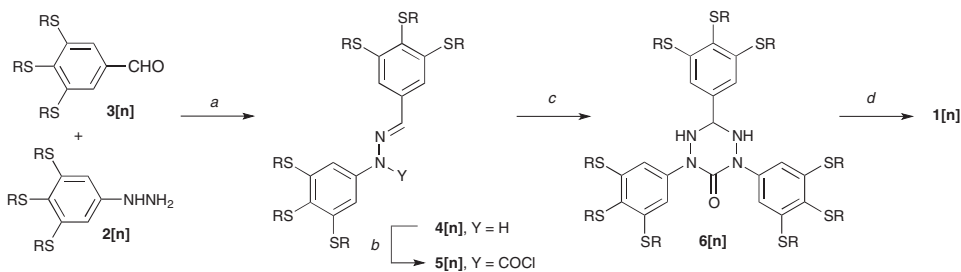
Scheme 1[a]

[a]Reagents and conditions: (a) EtOH, cat. AcOH, reflux; (b) $CO(OCCl_3)_2$, pyridine, CH_2Cl_2, rt; (c) **2[n]**, Et_3N, benzene, 50 °C; (d) PbO_2, Na_2CO_3, Toluene/MeCN or $K_3Fe(CN)_6$, Na_2CO_3 0.5 M, $[Bu_4N]^+Br^-$ (cat), CH_2Cl_2.
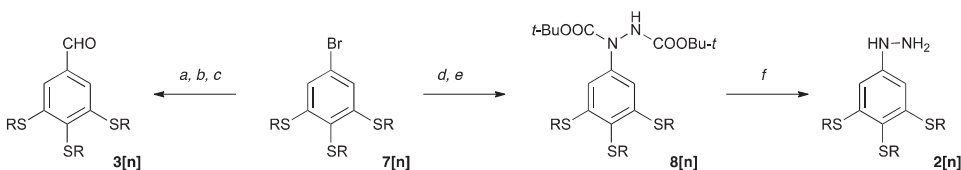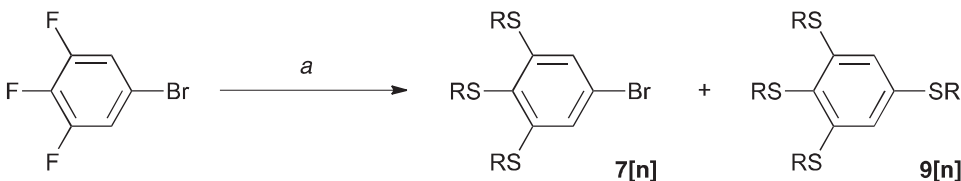
Scheme 2[a]

The requisite hydrazines **2[n]** and aldehydes **3[n]** were obtained from trialkylsulfanylbromobenzenes **7[n]** as shown in Scheme 2. Thus, bromobenzenes **7[n]** were treated with *t*-BuLi and the resulting aryllithiums were reacted with di-*t*-butyl azodicarboxylate (DTBAD) to give hydrazides **8[n]**. Hydrazines **2[n]** were prepared by removal of the *Boc* groups from hydrazides **8[n]** with five equivalents of TfOH in a CF_3CH_2OH/CH_2Cl_2 mixture at −40 °C and isolated as darkening viscous oils in purities >90% and yields of 60–86%.[13]

[a]Reagents and conditions: (a) *n*-BuLi, THF; (b) DMF; (c) aq HCl; (d) *t*-BuLi, THF; (e) *t*-BuOOCN = NCOOBu-*t*; (f) CF_3SO_3H, CF_3CH_2OH/CH_2Cl_2, −40 °C, <2 min.

Benzaldehydes **3[n]** were prepared in a routine way by lithiation of **7[n]** with *n*-BuLi and subsequent reaction of the aryllithium with dry DMF at −78 °C (Scheme 2).[14]

3,4,5-Trialkylsulfanylbromobenzes **7[n]** were obtained by reacting 1-bromo-3,4,5-trifluorobenzene with sodium alkanethiolate in dry DMSO or a DMSO/THF mixture for higher homologues (Scheme 3).[14] Tetraalkylsulfanylbenzenenes **9[n]** by products were formed in this reaction in the amounts of 20–40%, and they were separated by chromatography. However, complete purification of bromobenzenes **7[n]** was not necessary, since

Scheme 3[a]
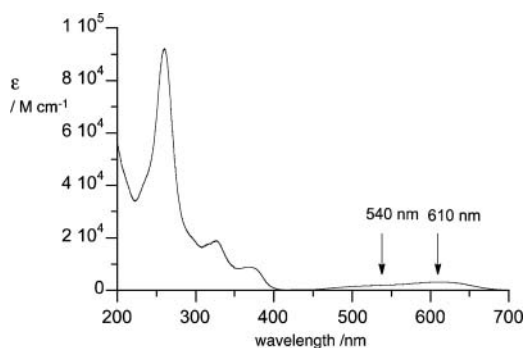
Figure 1 Electronic absorption spectrum of **1[8]** in hexane.

the by products **9[n]** are inert in the lithiation process and were readily separated from aldehydes **3[n]** or hydrazides **8[n]**.

[a]Reagents and conditions: (a) RSNa, DMSO, or DMSO/THF, 60–80 °C.

Electronic Absorption Spectroscopy

Hexane solutions of radicals are blue due to low-intensity absorption bands in the visible range with maxima at 540 nm and 610 nm (Figure 1). According to TD-DFT results for **1[1]** models, the absorption bands originate from several electronic transitions involving mainly the highest formally doubly occupied MOs, localized on the benzene rings, to the LUMO localized on the verdazyl unit (Figure 2). The excitation involving the SOMO to LUMO transition is calculated at 529 nm ($f = 0.03$) for **1[1]**.

Electrochemistry

Electrochemical analysis of **1[8]** in CH_2Cl_2 (10^{-3} M) showed two quasi-reversible redox pairs with potentials of $E^{0/+1}_{1/2} = +0.99$ V and $E^{0/-1}_{1/2} = -0.45$ V vs. SCE (Figure 3). The cell potential $E_{cell} = 1.43$ V is typical for other 6-oxoverdazyl derivatives.

β-LUMO, E = -0.11792   β-HOMO, E = -0.21537
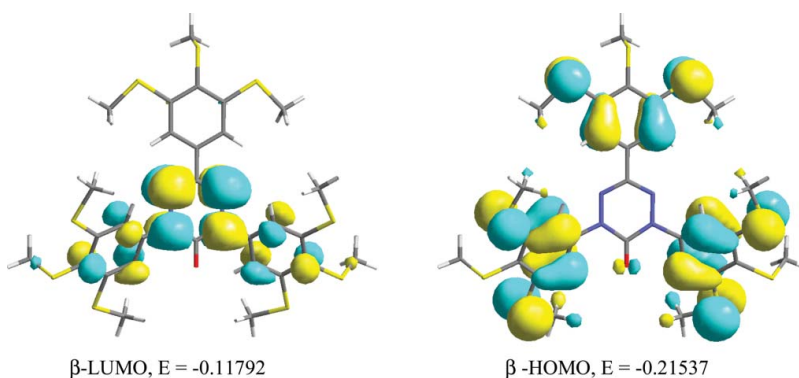
Figure 2 Contours and energies β-FMOs involved in the low energy excitations. (Color figure available online).
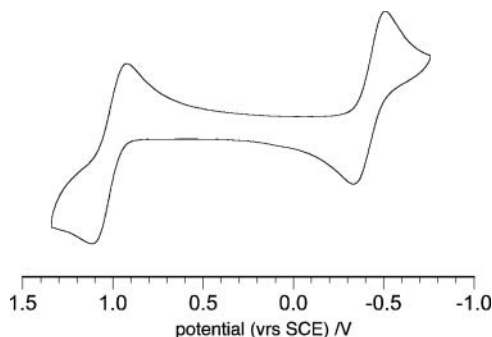
Figure 3 The cyclic voltammograms of **1[8]**: 1 mM, $[Bu_4N]^+[PF_6]^-$, 0.1 M, 100 mV s^{-1}.

Liquid Crystalline Behavior

Thermal analysis of a freshly crystallized sample of **1[8]** revealed a melting transition with a peak at 65 °C (Table 1, "heating 1" in Figure 4). Upon cooling the sample underwent a transition at 56 °C to a birefringent phase with a texture characteristic for a discotic columnar phase (Figure 5) that supercools to −40 °C. The monotropic phase undergoes transition to an isotropic phase at 60 °C on heating with an enthalpy comparable to that recorded on cooling. Crystalline polymorph of **1[8]** obtained from melt is different from that obtained from solutions. It melts with a peak at 52 °C forming an enantiotropic phase with a transition to the isotropic phase at 60 °C ("heating 2" in Figure 4). Similar mesogenic behavior is observed for **1[6]** and **1[10]** homologues (Table 1), while compound **1[12]** does not exhibit liquid crystalline properties.

Powder X-ray diffraction (XRD) analysis for the three lower homologues of **1[n]** revealed formation of a columnar rectangular phase (*Col*$_r$) consistent with the polarized microscopy texture (Figure 5). The fast-cooled samples gave XRD patterns with two sharp diffraction signals in the small angle region that can be indexed as (11) and (02), and a typical broad halo at 4.2 Å in the wide-angle region (Figure 6, Table 2). Upon further cooling, the sample crystallized, that manifested itself in significant changes in the XRD patterns; the sharp signals disappeared and pronounced small-angle scattering of the X-ray beam was observed instead. Larger crystallites (or another crystalline polymorph) could however be observed for slowly cooled samples-in this case the diffraction patterns exhibited similar features to that of the fast-cooled sample in columnar phase with additional low intensity sharp reflections in the entire range of the diffractogram.

Table 1 Transition temperatures (°C) for **1[n]**[a]

n	1a[n]
6	Cr 39 Col$_r$ 50 I
8	Cr 62 (Col$_r$ 60) I
10	Cr 62 (Col$_r$ 55) I
12	Cr 63 I

[a]Determined by DSC (5 K min^{-1}) in the heating mode: Cr = crystalline; Col$_r$ = columnar rectangular; I = isotropic.
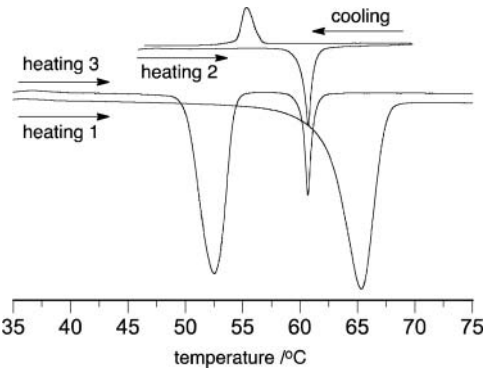
Figure 4 DSC traces of **1[8]**. The heating and cooling rates are 5 K min^{-1}.
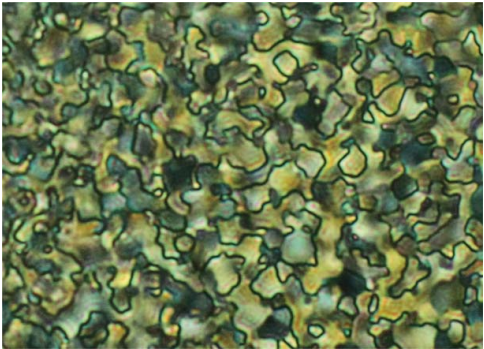
Figure 5 Optical textures of a *Col*$_r$ phase of **1[8]** upon fast cooling. (Color figure available online).

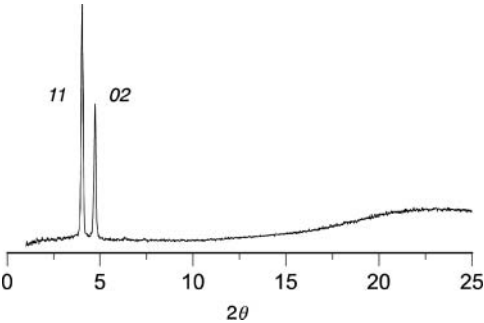**Figure 6** 2D XRD pattern for **1[8]** at 25 °C.

Table 2 X-ray diffraction data for **1[n]**

n	Temp /°C	Miller indices hk	1[n] d spacing (Å)	Latticeparameters (Å)
6	30	11	19.7	a = 24.1
		02	17.1	b = 34.2
		11	21.9	a = 26.9
8	30	02	18.8	b = 37.6
		11	23.5	a = 29.4
10	30	02	19.6	b = 39.2

Magnetic Properties

Magnetization studies of **1[8]** (at 200 Oe) revealed paramagnetic behavior in all phases. The effective magnetic moment (μ_{eff}) for **1[8]** in the crystalline phase was found to be 1.620 ± 0.03 in a temperature range of 310–345 K, which is close to the value of 1.732 for an ideal paramagnet and corresponds to $93 \pm 3\%$ of spins (Figure 7). The number of spins increased to $95 \pm 2\%$ at about 65 °C, which coincides with melting to an isotropic phase, Cr→I. No abrupt changes of magnetization were observed at the phase transitions upon cooling (I→Col_{r}) or heating (Col_{r}→I), and the number of spins remained approximately constant at $95 \pm 2\%$.

Cooling of the samples from the isotropic phase to 2 K in magnetic field showed that molar susceptibility χ_m is well described by Curie law down to 200 K (Figure 8). At lower temperatures antiferromagnetic interactions gradually reduce the observed magnetization. These results indicate that the alkylsulfanyl groups prevent effective intermolecular close π–π contacts, and the unpaired electrons remain largely isolated either in the rigid or fluid phases. This is consistent with results of molecular modeling for **1[8]**, which show alkyl chains effectively preventing blocking access to the verdazyl core (Figure 9).

Photovoltaic Properties

Time-of-flight (TOF) measurements found positive charge carrier (hole) mobility (μ_h) in a fast-cooled, unaligned multidomain sample of **1[8]** to be 1.52×10^{-3} cm^2 V^{-1} s^{-1} at 40 °C (Figure 10), which is in the range of typical values of 10^{-4}–10^{-1} cm^2 V^{-1} s^{-1}.
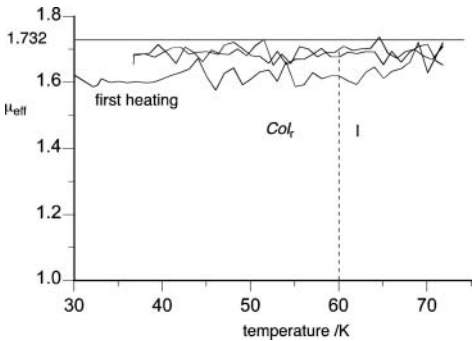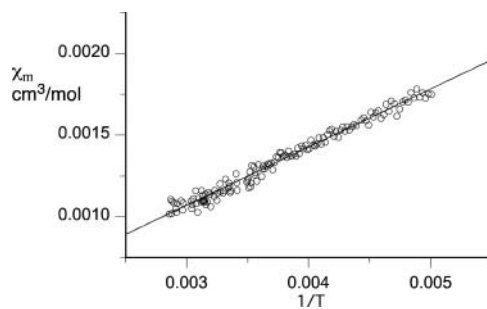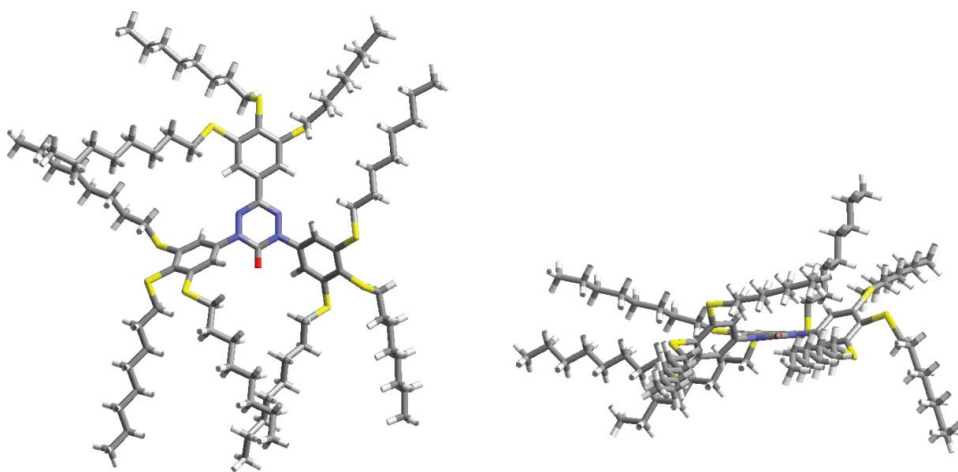

Figure 7 μ_{eff} vs. T plot for **1[8]**. H = 200 Oe.

Figure 8 Paramagnetic molar susceptibility χ_m vs. $1/T$ plot after diamagnetic correction. C = 0.357(1) cm^3 K mol^{-1}. H = 200 Oe.

Figure 9 Two views of a molecule of **1[8]** optimized with the UFF algorithm. Alkyl chains are in the all-*trans* conformation. (Color figure available online).
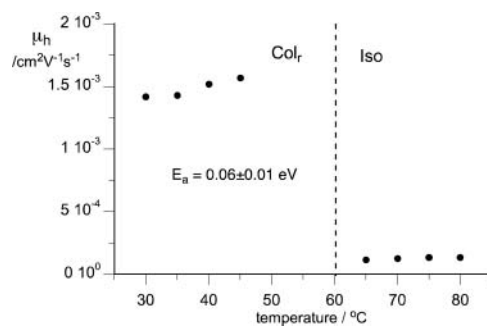
Figure 10 The temperature dependence of positive carrier mobility obtained by the TOF method for **1[8]** at 337 nm. Electric field strength 40 kVcm^{-1}.

The Arrhenius analysis of μ_h at several temperatures gave the activation energy $E_a = 0.06 \pm 0.01$ eV and is consistent with a hopping transport mechanism.

SUMMARY

The first series of liquid crystalline derivatives of the verdazyl radical has been synthesized and characterized.[12] Compounds in series **1[n]** containing alkylsulfanyl chains exhibit the *Col*r phase, however magnetic analysis demonstrated that the verdazyl units are largely isolated even in the solid phase. We have demonstrated charge photogeneration and its transport in a liquid crystalline radical, which is comparable to that in other discotic mesogens. Further studies of liquid crystalline derivatives of the verdazyl, such as oxygen analogues of **1[n]**,[16] are in progress in our laboratory.

REFERENCES

1. For example: (a) van de Craats, A. M.; Stutzmann, N.; Bunk, O.; Nielsen, M. M.; Watson, M.; Müllen, K.; Chanzy, H. D.; Sirringhaus, H.; Friend, R. H. *Adv. Mater.* **2003,** 15, 495-499 (b) Dong, S.; Tian, H.; Song, D.; Yang, Z.; Yan, D.; Geng, Y.; Wang, F. *Chem. Commun.* **2009,** 3086-3088.

2. Schmidt-Mende, L.; Fechtenkötter, A.; Müllen, K.; Moons, E.; Friend, R. H.; MacKenzie, J. D. *Science* **2001,** 293, 1119-1122.

3. Kumar, S. *Curr. Sci.* **2002,** 82, 256-257.

4. Kaafarani, B. R. *Chem. Mater.* **2011,** 23, 378-396.

5. Haddon, R. C. *Aust. J. Chem.* **1975,** 28, 2343-2351.

6. Castellanos, S.; López-Calahorra, F.; Brillas, E.; Juliá, L.; Velasco, D. *Angew. Chem. Int. Ed.* **2009,** 48, 6516-6519.

7. (a) Wiley, P. F. In: *Chemistry of 1,2,3-Triazines and 1,2,4-Triazines, Tetrazines and Pentazines*; Willey & Sons: New York, **1978,** pp. 1225-1246; (b) Koivisto, B. D.; Hicks, R. G. *Coord. Chem. Rev.* **2005,** 249, 2612-2630, and references therein (c) Hicks, R. G. (Ed). In: *Stable Radicals: Fundamentals and Applied Aspects of Odd-Electron Compounds*; Wiley & Sons, **2010**, pp. 245-280, and references therein.

8. (a) Neugebauer, F. A. *Tetrahedron* **1970,** 26, 4853-4857 (b) Gilroy, J. B.; McKinnon, S. D. J.; Koivisto, B. D.; Hicks, R. G. *Org. Lett.* **2007,** 9, 4837-4840 (c) Chemistruck, V.; Chambers, D.; Brook, D. J. R. *J. Org. Chem.* **2009,** 74, 1850-1857.

9. (a) Mukai, K.; Shiba, D.; Yoshida, K.; Mukai, K.; Hisatou, H.; Ohara, K.; Hosokoshi, Y.; Azuma, N. *Bull. Chem. Soc. Jpn.* **2005,** 78, 2114-2123 (b) Chahma, M.; Macnamara, K.; van der Est, A.; Alberola, A.; Polo, V.; Pilkington, M. *New. J. Chem.* **2007,** 31, 1973-1978.

10. (a) Toichi, T.; Teki, Y. *Polyhedron* **2005,** 24, 2337-2340 (b) Mihara, N.; Teki, Y. *Inorg. Chim. Acta* **2008,** 361, 3891-3894.

11. Ciofini, I.; Adamo, C.; Teki, Y.; Tuyeras, F.; Laine, P. P. *Chem. Eur. J.* **2008,** 14, 11385-11405.

12. Jankowiak, A.; Pociecha, D.; Szczytko, J.; Monobe, H.; Kaszyński, P. *J. Am. Chem. Soc.* **2012,** 134, 2465-2468.

13. Jankowiak, A.; Kaszynski, P. *Beils. J. Org. Chem.* **2012,** 8, 275-282.

14. Jankowiak, A.; Dębska, Z.; Kaszyński, P.; Romański, J. *J. Sulfur Chem.* **2012,** 33, 1-7.

15. Milcent, R.; Barbier, G.; Capelle, S.; Catteau, J.-P. *J. Heterocyc. Chem.* **1994,** 31, 319-324.

16. Jankowiak, A.; Pociecha, D.; Monobe, H.; Szczytko, J.; Kaszyński, P. *Chem. Commun.* **2012,** 48, 7064-7066.